红外与激光工程
INFRARED AND LASER ENGINEERING
EI, SCOPUS, CSCD等收录期刊

生物气溶胶荧光激光雷达技术研究进展

栗喆锴　唐大为　吴柯南　魏天问　夏海云

Research progress of bioaerosols fluorescence lidar technology

LI Zhekai, TANG Dawei, WU Kenan, WEI Tianwen, XIA Haiyun

在线阅读 View online: https://doi.org/10.3788/IRLA20240580

您可能感兴趣的其他文章

Articles you may be interested in

大气多参数激光雷达在化工园区的安全环保和碳监测中的应用

Application of atmospheric multi-parameter lidar in safety, environmental protection and carbon dioxide monitoring in chemical industrial parks

红外与激光工程. 2024, 53(5): 20240068　https://doi.org/10.3788/IRLA20240068

亚稳态氦激光雷达的研制进展

Progress on developing metastable helium Lidar

红外与激光工程. 2020, 49(S2): 20200323　https://doi.org/10.3788/IRLA20200323

底层大气探测激光雷达国内研究现状与进展（特邀）

Research status and progress of Lidar for atmosphere in China (*Invited*)

红外与激光工程. 2021, 50(3): 20210032　https://doi.org/10.3788/IRLA20210032

探测气溶胶-水汽的拉曼-米散射激光雷达系统

Raman-Mie scattering lidar system for detection of aerosol and water vapor in the atmosphere

红外与激光工程. 2023, 52(4): 20220484　https://doi.org/10.3788/IRLA20220484

星载云气溶胶激光雷达光机系统结构及研究进展

Opto-mechanical system structure and research progress of space-borne lidar for cloud-aerosol

红外与激光工程. 2020, 49(8): 20190501　https://doi.org/10.3788/IRLA20190501

基于激光雷达的区域大气颗粒物探测

Detection of regional atmospheric particulate matter based on lidar

红外与激光工程. 2020, 49(S2): 20200324　https://doi.org/10.3788/IRLA20200324

生物气溶胶荧光激光雷达技术研究进展

栗喆锴[1], 唐大为[2], 吴柯南[1,2], 魏天问[1], 夏海云[1,2*]

(1. 南京信息工程大学 大气物理学院, 江苏 南京 210044;
2. 中国科学技术大学 地球和空间科学学院, 安徽 合肥 230026)

摘　要: 生物气溶胶是大气中重要的悬浮颗粒,包含花粉、病毒、细菌等成分,对环境气候变化、公共卫生及国防安全等领域具有重要影响。激光雷达凭借对气溶胶颗粒的高灵敏度和高精度时空分布的探测能力,成为远程探测生物气溶胶的重要技术手段,在生物战剂预警、花粉监测及大气环境研究等领域展现出广阔应用潜力。基于不同原理的激光雷达在生物气溶胶探测方面取得了显著进展,其中激光诱导荧光 (LIF) 激光雷达的应用最为广泛。文中以波长为主线,系统综述了 LIF 激光雷达在生物气溶胶探测中的研究现状,归纳了其技术特点与局限性,并展望了其在该领域的未来应用前景。

关键词: 生物气溶胶;　激光雷达;　大气遥感;　激光诱导荧光

中图分类号: P412.25　　**文献标志码:** A　　**DOI:** 10.3788/IRLA20240580

引用格式: LI Zhekai, TANG Dawei, WU Kenan, et al. Research progress of bioaerosols fluorescence lidar technology[J]. ***Infrared and Laser Engineering***, 2025, 54(6): 20240580.
栗喆锴, 唐大为, 吴柯南, 等. 生物气溶胶荧光激光雷达技术研究进展[J]. 红外与激光工程, 2025, 54(6): 20240580.

0　引　言

气溶胶,指的是被动悬浮在气体介质中的液态或固态 (或两者同时存在) 的粒子。而生物气溶胶,广义上来说指的是来自生物系统的气溶胶,是由有机物质组成的,通常为蛋白质、脂质和糖类的混合物[1];而狭义上来说,生物气溶胶通常指初次生物气溶胶颗粒 (PBAP),即从生物圈直接排放到大气中的颗粒,比如空气中悬浮的花粉、病毒和微生物碎片等[2]。生物气溶胶尺寸千差万别,有小到 0.001 μm 的分子团簇,也有大到 100 μm 的花粉或藻类[3],其主要来源包括土壤、灰尘、江河湖海以及动植物等[4]。相关实验观测结果显示,城市和农村中生物气溶胶的数浓度平均为 1.9 cm^{-3},约占大气数浓度的 30%,平均体积浓度约占大气总体积浓度 15%[5]。

生物气溶胶在多个领域具有重要的研究意义。在环境与气候方面,生物气溶胶作为冰核参与云的形成过程,研究表明,生物气溶胶可以在较暖条件下活化,在人工影响天气催化剂的研究中展现出重要的应用潜力[6]。作为一种重要的气溶胶类型,生物气溶胶也会通过云-气溶胶相互作用影响全球的辐射平衡[7]。此外,生物气溶胶和沙尘气溶胶的增加可能会导致大气污染,同时也可能会促进生物生产力,影响海洋碳吸收[8]。生物气溶胶还可能会被输送到较高的海拔高度,并在风力或沙尘暴的作用下传播到更远的地区,从而对大气环境产生更广泛的影响[9]。在公共卫生方面,2019 年新型冠状病毒肺炎疫情 (COVID-19) 期间,病毒的气溶胶传播引发了广泛关注[10-14]。此外,研究表明,吸入空气中的花粉是过敏性疾病患者症状的重要诱因之一[15]。在国防安全方面,生物武器通过气溶胶传播可引发大规模感染,并且在短时间内难以被察觉[16]。因此,如何快速识别潜在的危险生物气溶胶,提高对生物武器袭击的检测能力,对于加强国防和反恐工作具有重要意义[17]。

激光雷达是一种先进的大气遥感探测仪器,对大气中的颗粒物具有高度敏感性,能够精确获取颗粒源的时空分布信息,是远程探测生物气溶胶的重要技术

收稿日期: 2024−12−13;　**修订日期:** 2025−02−20

作者简介: 栗喆锴,男,硕士生,主要从事激光雷达技术方面的研究。

导师(通讯作者)简介: 夏海云,男,教授,博士,主要从事激光雷达技术方面的研究。

手段[18]。例如，生物气溶胶攻击可能引发大规模感染，因此迫切需要快速检测大气中的生物气溶胶以采取有效应对措施。传统的点式检测方法需要先采集样本并在实验室分析，通常耗时 12~36 h，而基于光学系统的激光雷达可以实现实时、远距离检测[18]，从而提供早期预警，为防范措施争取宝贵时间。此外，激光雷达可用于大范围的花粉观测，不仅为研究花粉分布规律提供支持[19]，还为评估花粉对人类致敏作用的临床影响提供基础数据[20]。地基激光雷达具备长期稳定观测的能力，能够积累大量数据[21]，在生物气溶胶时空分布的统计研究中具有重要意义。

目前，用于生物气溶胶远程探测的激光雷达主要基于四种原理：偏振 (Polarization)、激光诱导击穿光谱 (LIBS)、差分散射 (DISC) 和激光诱导荧光 (LIF)。偏振激光雷达在区分大气中球形和非球形粒子方面表现出色，被广泛应用于大气气溶胶和云的探测[22]。随后，研究者将该技术应用于生物气溶胶的远程探测中。例如，芬兰[23]、韩国[24] 和美国[20] 的研究者观测到了高退偏比的花粉信号；中国[25]、加拿大[26] 和美国[27] 的研究者则开展了生物战剂模拟物的偏振探测研究。LIBS 是一种强大实时的材料元素分析工具，在爆炸物检测领域有广泛的应用[28]。加拿大[29-30] 和美国[31-32] 的研究者进一步改进了 LIBS 技术，开展了远程生物气溶胶探测实验，但有效探测距离较近 (通常在 100 m 以内)。DISC 技术主要通过多种不同波长的后向散射差异分析气溶胶的粒径及其它光学特征[33]。结合不同的算法与激光雷达系统，加拿大[34] 和美国[35-36] 的研究者进行了远程生物气溶胶探测实验。LIF 激光雷达可以获取生物气溶胶的特征荧光信号，具有识别与分类的潜力，是生物气溶胶远程探测领域研究最为广泛的技术，具有良好的发展前景。

文中聚焦于 LIF 激光雷达在生物气溶胶探测领域的研究进展，阐述其基本原理，并基于不同激发波长梳理远程探测的研究现状。最后，总结其技术特点与局限性，并展望未来应用前景。

1　LIF 激光雷达的基本原理与分析

1.1　LIF 激光雷达的基本原理

利用激光激发物质并引发其发射荧光的过程被称为激光诱导荧光 (LIF)，由于生物荧光团的荧光较弱且在空气中的浓度较低，激发辐射需具备足够的能量，因此通常选用激光作为激发光源[37]。生物气溶胶中富含多种荧光团，如酪氨酸、苯丙氨酸和还原型辅酶 Ⅰ 等，这些荧光团在紫外光的照射下会自发发射荧光，因此，LIF 技术可用于生物气溶胶的探测[38]。如图 1 所示，有研究者使用 266 nm 激光激发单颗粒的荧光团，结果显示，不同荧光团产生的荧光光谱具有显著的特征差异[39]。通过分析这些荧光光谱，研究人员能够对不同类型的荧光团进行相对准确的分类[40]。

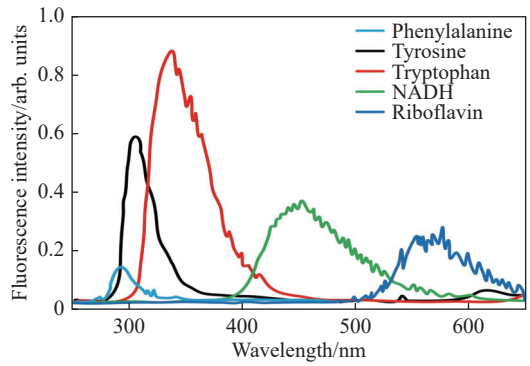

图 1　使用 266 nm 激发的生物颗粒中常见荧光物质的荧光光谱[39]

Fig.1　266-nm-excited fluorescence spectra of common fluorophores found in biological particles[39]

基于此，理论上可以将 LIF 技术与激光雷达系统相结合，通过发射特定的激发波长并使用光电探测器接收对应波段的荧光，得到光谱信号或对光谱进行积分得到光谱积分信号，从而实现对大气中生物气溶胶的远程探测[41]。利用激光雷达方程，可以校正大气传输引起的波长透过率不一致性，从而得到荧光后向散射系数。还可以与气体拉曼信号，如氮气拉曼信号相比较，进行归一化处理。VESELOVSKII 等利用氮气拉曼信号反演出积分荧光后向散射系数，并将其作为对气溶胶粒子分类的一个有效依据[7]，RAO 等还推导出了生物气溶胶浓度信息[41]。还有大量的研究者结合光谱库数据，并使用了支持向量机、主成分分析和光谱角度映射等算法对生物气溶胶进行了识别与分类，得到了较好的结果。SHANGGUAN 等还实现了水下浮游生物的远程探测，并进行了船载探测实验[42-44]。除了上述两种信号，还有大量探测浮油相关方向的研究者使用了基于时间分辨的荧光信号[45-47]，FELLNER 等将此信号应用在了生物气溶胶探测系统中，提高了

该系统的分类能力[48]。表 1 列出了目前 LIF 激光雷达在生物气溶胶探测领域使用的主要激发波长 (OPO 表示光参量震荡器, BBO 表示一种非线性晶体)。

表 1 LIF 激光雷达主要的激发波长、相关的激光器种类和主要参考文献

Tab.1 Main excitation wavelengths, related laser types and main references for LIF lidar

Main excitation wavelength/nm	Lasers	Main references
266	Nd:YAG	[41,49-50]
280	Nd:YAG-OPO	[51]
294	Nd:YAG-BBO	[52]
355	Nd:YAG	[7,53-54]
351	Excimer laser	[55-56]
405	Semiconductor laser	[57]

1.2 LIF 激光雷达激发波长的选择

激发荧光的波长是影响 LIF 激光雷达探测距离和性能的关键因素之一[58], 在选择波长时需以目标物的荧光特性为主, 进行综合考虑。研究表明, 具有较高荧光效率的有机分子通常包含交替双键或芳香环等共轭结构[59]。这类分子的 S1 和 S0 能级之间的能量差通常对应 200 nm 至 1 μm 波长光子的能量; 而不含共轭结构的有机分子, 其吸收阈值一般低于 200 nm 光子的能量, 但此能量已超过大多数化学键的解离能, 因此在高能辐射照射下, 这些分子可能在荧光激发前发生解离[59-60]。许多生物分子 (例如, 广泛存在于某些细菌、病毒和毒素中的色氨酸及 NADH 等[61]) 含有共轭结构, 是优良的荧光团。激发-发射矩阵 (EEM) 是由激发波长和相应荧光发射光谱构成的三维矩阵, 为 LIF 激光雷达的波长选择提供了重要依据[61]。图 2 展示了两种重要荧光团的 EEM图, 为确保激发光谱的代表性, 如果目标物为色氨酸, 则激发波长应选择在 300 nm 以下[59]。

上述研究主要针对单一荧光团, 而在实际激光雷达大气观测中, 由于生物气溶胶的成分复杂, 激光激发产生的荧光光谱通常是多种荧光团混合信号, 这给激光雷达对生物气溶胶的分类与识别带来了挑战[62]。SAARI 等的研究表明, 大气中细菌和真菌的荧光特性存在显著差异: 例如, 在 280 nm 激发下, 300~400 nm 的发射波段 (色氨酸和酪氨酸) 与细菌的荧光特性有关; 而在 410 nm 激发下, 500~650 nm 的发射波段 (核黄素等) 与真菌的荧光特性有关[63]。在设计 LIF 激光雷达时, 应综合考虑目标物的荧光特性及探测需求, 选择最适合的激发波长[64]。由于 Nd:YAG 激光器具有性能优越、操作简便、商业化程度高且成本较低等优点, 在考虑荧光特性的基础上, 266 nm 和 355 nm 成为常用的激发波长 (分别是 Nd:YAG 激光器基频的三倍频和四倍频)。其中, 266 nm 主要用于激发细菌细胞壁内氨基酸的荧光[58], 其激发出的荧光光谱较 355 nm 更具多样性[65]; 而 355 nm 则主要用于激发 NADH 的荧光[52]。

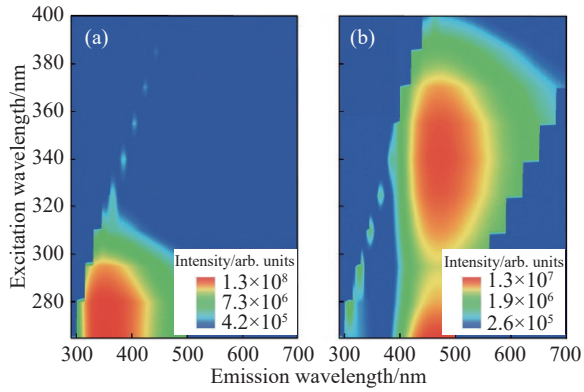

图 2 荧光团的激发-发射矩阵图。(a) 色氨酸; (b) 还原性辅酶 I(NADH)[59]

Fig.2 Excitation-emission matrix of fluorophores. (a) Tryptophan; (b) Reduced coenzyme I(NADH)[59]

1.3 LIF 激光雷达探测器的选择

为了获取荧光光谱, 大多数 LIF 激光雷达系统将光谱仪与以下两种类型的光电探测器结合: (1) ICCD, 该装置通过光纤耦合系统将图像增强器与光电耦合器件 (CCD) 结合。图像增强器通常由光电阴极、微通道板 (MCP) 和荧光屏三部分组成。其中, 光电阴极能够将入射的光子转化为电子, 这些电子在加速过程中进入 MCP。在 MCP 施加的高电压作用下, 入射电子激发更多电子, 从而实现信号放大[66]; (2) 多阳极光电倍增管 (MAPMT), 由阴极、倍增极链和分段阳极组成, 其优化的结构使得入射到阴极上的光子的空间分布能够真实地再现为阳极处的信号[67]。上述两种探测器均具备单光子探测能力, 但各有优缺点。ICCD

具有更高的光谱分辨率，但灵敏度较低，读取速度较慢，因此在捕获距离分辨信号时存在一定局限性[67-68]；相比之下，MAPMT 的光谱分辨率较低，但其典型增益较大，响应速度快，能够获取较高距离分辨率的信号[68-69]。

除了分析生物气溶胶的荧光光谱外，还可以使用单个 PMT 探测波长积分的荧光信号。RAO 等利用荧光积分信号反演了不同距离处生物气溶胶的数浓度分布[41]。VESELOVSKII 等利用荧光积分信号计算出了一种强度量 (荧光容量)，作为大气气溶胶分类和反演的参数[70]。PMT 还可用于弹性信号探测，获取目标气溶胶云团的距离和深度信息，以便控制 ICCD 和 MAPMT 的门控时间，在感兴趣的距离处收集荧光信号[71]。

2　LIF 激光雷达生物气溶胶探测的研究现状

图 3 所示的相关研究机构如下：德国气象局 (DWD)、德国明斯特 CBRN 研究中心 (WIS)、德国宇航局 (DLR)、英国国防科技实验室 (Dstl)、法国里尔大学 (ULille)、雅典国家技术大学 (NTUA)、以色列生物研究所 (IIBR)、挪威国防研究院 (FFI)、波兰华沙董布罗夫斯基军队技术学院 (MUT)、瑞典国防研究局 (FOI)、爱沙尼亚共和国 LDI Innovation 公司、俄罗斯科学院普罗霍夫普通物理研究所 (GPI RAS)、印度国防研究与发展组织 (DRDO)、俄罗斯科学院大气光学研究所 (IAO SB RAS)、中国人民解放军军事医学科学研究院 (AMMS)、北京合鲸科技发展有限公司 (Bewhale)、北京理工大学 (BIT)、北方民族大学 (NMU)、中国人民解放军陆军炮兵防空兵学院 (AAAAD)、中国科学技术大学 (USTC)、西安理工大学 (XAUT)、武汉大学 (WHU)、兰州大学 (LZU)、韩国釜庆大学 (PKNU)[72]、日本信州大学 (Shinshu University, 图 3 中用 SU 代替)、日本气象研究所 (MRI)、日本国立环境研究所 (NIES)、加拿大国防研究与发展部 (DRDC)、美国陆军埃奇伍德研究发展与工程中心 (ERDEC)、美国陆军生化防御指挥部 (CBDC)、美国科学与工程服务公司 (SES)、美国杜格威武器试验场 (DPG)。表 2 展示了不同研究机构 LIF 激光雷达的部分参数，其中第二列的 cw 表示连续激光器，其余均为脉冲激光器。第四列代表研究该激光雷达的主要探测目标，其中 BWA 代表生物战剂，是众多国防机构的重要探测目标，在外场测试实验中一般用生物战剂模拟物来代替。下文将按照波长分类，对部分研究机构的成果进行介绍。

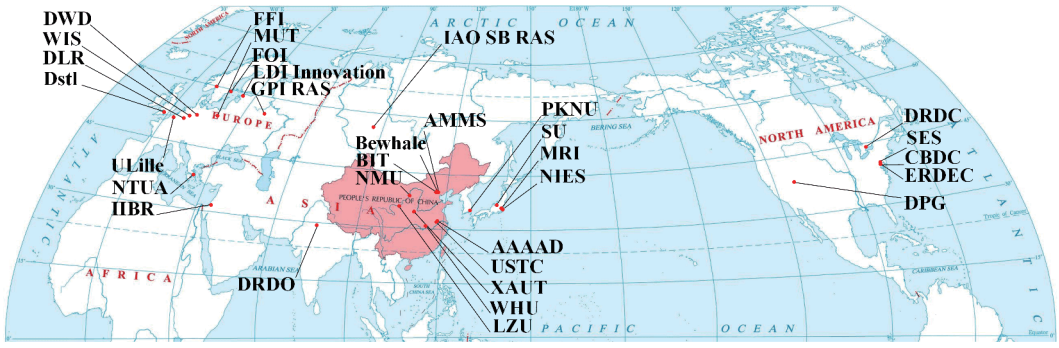

图 3　相关研究机构的地理分布图。基于标准地图服务系统提供的地图制作，审图号为 GS(2020)4388，截取了北半球部分。地图上的点标注了相关研究机构的大致地理位置，所用数据来源于 Microsoft 公司提供的 Bing Maps 服务

Fig.3　Geographic distribution map of relevant research institutions. This map is based on the map provided by the Standard Map Service, review number GS(2020)4388, with the northern hemisphere portion intercepted. The dots on the map indicate the approximate geographic locations of the relevant research institutions, and the data used were obtained from the Bing Maps service provided by Microsoft Corporation

2.1　266 nm 单激发波长

1991 年，ERDEC 测试了一套紫外荧光激光雷达系统。该系统的单脉冲能量范围为 170~200 mJ，重频为 10 Hz，配备三个数据收集通道，分别用于实时监

表 2 各个研究机构 LIF 激光雷达的相关参数表

Tab.2 Table of relevant parameters of LIF lidar from various research institutes

Abbreviations of research institutes	Laser parameters	Detector	Target	Main references
AAAAD	5 mJ@266 nm, 10 mJ@355 nm	32-ch PMT	BWA	[73-74]
AMMS	100 mW@405 nm(cw)	PMT	BWA	[57]
Bewhale	266 nm, 355 nm	PMT, ICMOS	BWA	[75]
BIT	20/30 mJ@355 nm	PMT	Air pollution, Tryptophan	[76-77]
DLR	10 mJ@280 nm, 10 mJ@355 nm	ICCD	Bacteria	[51]
DRDC	100 μJ/24 mJ@355 nm	32-ch PMT/ ICCD	BWA	[78]
	150-200 mJ@351 nm	ICCD	BWA	[56]
DRDO	10-70 mJ@266 nm	ICCD	BWA	[79]
	5-35 mJ@355 nm	CCD	BWA	[80]
Dstl	40 mJ@266 nm	10-ch PMT	BWA	[81]
DWD	300/450 mJ@355 nm	PMT/ Multi-ch PMT	Raman signal's influence	[54,82]
ERDEC	200 mJ@266 nm	PMT/ICCD	BWA	[83]
FFI	170 mJ@355 nm	ICCD	BWA	[84]
	3-5 mJ@294 nm, 30 mJ@355 nm	ICCD	BWA	[52]
FOI	20/50 mJ@355 nm	32-ch PMT	BWA	[85-86]
IAO SB RAS	60 mJ@266 nm	ICCD	BWA	[87]
IIBR	<1/20 mJ@266 nm	ICCD	BWA & scavenging process	[50,88]
LDI Innovation	5 mJ@248 nm, 2 mJ@351 nm	Gated linear detector	Bacteria	[55]
LZU	355 nm	32-ch PMT	Pollutant, dust	[89]
	80 mJ@355 nm	64-ch PMT	Humic-like substances	[90]
MRI	260 mJ@355 nm	ICCD	Raman signal's influence	[91]
MUT	266 nm, 355 nm	28-ch PMT	BWA	[92]
NIES	100 mJ@355 nm	32-ch PMT	Air-pollution aerosols, dust	[93]
NTUA	24.7 mJ@266 nm	32-ch PMT	Pollen, Fungal	[49]
SES	1.5 mJ@355 nm	PMT	BWA	[94]
	5 mW@375 nm(cw)	PMT	BWA	[95]
Shinshu University	10 mJ@355 nm	ICCD	Pollen	[53]
	0.3 mW@325 nm, 34.3 mW@405 nm, 17.5 mW@455 nm, 30 mW@520 nm(cw)	PMT	Pollen	[96]
ULille	70/80 mJ@355 nm	PMT	Pollen, dust, smoke plume, atmosphere aerosols	[7,97]
USTC	>200 mJ@355 nm	32-ch PMT	Fluorescent aerosol	[98]
WHU	100 mJ@355 nm	32-ch PMT	Raman signal's influence	[99]
XAUT	60 mJ@266 nm	PMT	Fluorescent aerosol	[41]

测 266 nm 的弹性后向散射、300~400 nm的总荧光、以及通过 ICCD 记录的 250~500 nm 范围内的荧光光谱信号[100]。测试结果表明，该系统在夜间能够在 3 km 处探测到枯草芽孢杆菌的极限浓度为 500 mg/m^3[83]。

1999 年，ERDEC 开发了一款可搭载于无人机的双波长 (266 nm 和 1 064 nm) 激光雷达系统，增加了 LIF 激光雷达的机动性[101]。

2015 年，IIBR 使用其研制的紧凑型 LIF 激光雷

达系统 (单脉冲能量为 20 mJ, 重频为 10 Hz, 配备 ICCD 探测器) 在距离 200 m 的云室内测量到了大量荧光光谱, 并通过光谱角映射 (SAM) 分析算法区分了色氨酸、乳清蛋白及常见背景的荧光信号[102]。到 2020 年, 该激光雷达在白天最远探测到了 2.5 km 处的生物气溶胶光谱信号, 如图 4 所示[50]。2023 年, 该研究所将脉冲能量降低至 1 mJ 以下, 并对含有生物气溶胶的水滴进行了实时观测, 为研究生物气溶胶的清除过程提供了新方法[88]。

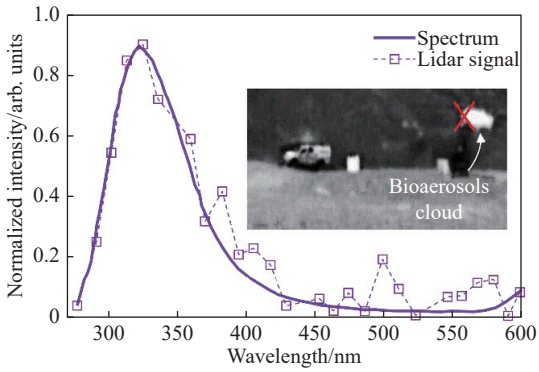

图 4　正午时分, 激光雷达在 2.5 km 处测到卵清蛋白 (OV) 的荧光光谱 (虚线) 和 OV 光谱库中的光谱 (实线), 插图中的叉号标示了激光雷达视场的指向位置[50]

Fig.4　Fluorescence spectrum of ovalbumin (OV, purple dashed line) and spectrum from the OV spectral library (purple solid line) were measured by lidar at 2.5 km at midday, and the cross in the inset is the lidar field of view pointing to the white bioaerosols cloud [50]

2018 年, XAUT 在前期一系列数值仿真的基础上[103-104], 研制了一台激光雷达, 该雷达单脉冲能量为 60 mJ, 重频为 10 Hz, 使用 PMT 收集 310~440 nm 范围内的总荧光信号。在测试中, 该雷达观测到了 1 km 高度内明显的荧光气溶胶层, 并通过荧光激光雷达方程成功反演出荧光气溶胶的数浓度[41]。

2019 年, NTUA 的激光雷达遥感小组开发了一台 LIF 激光雷达, 单脉冲能量约为 24.7 mJ, 重频为 10 Hz, 用于低空 (主要在 1 km 以下) 对当地常见生物气溶胶 (如花粉) 进行光谱分析。该研究小组开发了一套反演算法, 将原位荧光光谱数据和激光雷达数据结合分析, 从而判断不同种类生物气溶胶对观测结果的贡献。生物气溶胶的相对贡献在研究期间存在显著变化, 这一结果为相关疾病的预防提供了重要的数据支持[49]。

2.2　355 nm 单激发波长

2.2.1　355 nm 激发产生的水汽拉曼信号对荧光的影响

2005 年, DWD 和阿尔弗雷德瓦格纳极地海洋研究所 (AWI) 在使用多波长移动气溶胶拉曼激光雷达 (MARL) 观测水汽和气溶胶时, 发现水汽 407 nm 拉曼通道中异常高的非弹性散射信号。研究认为, 这一现象是由生物质燃烧气溶胶 (BBA) 在激发后产生的荧光干扰所致[82]。

2022 年, WHU 课题组在使用光谱分辨拉曼激光雷达 (SRRL) 时, 也观测到了荧光信号。如图 5 所示, 荧光信号随波长变化较小, 采用线性拟合方法, 将荧光光谱与水汽光谱从收集的总信号中有效分离。这一方法在有荧光气溶胶的情况下, 显著提升了水汽信号的测量准确性[99]。

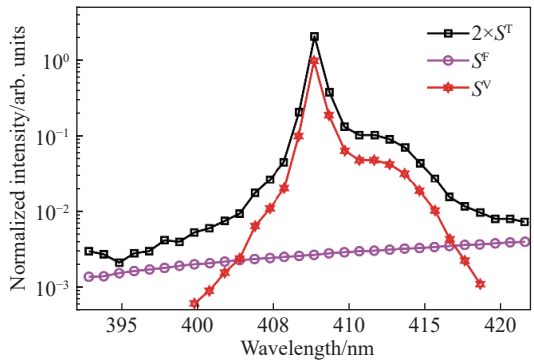

图 5　由激光雷达在 1.5~2.0 km 高度范围内积累光子得出的总归一化光谱 S^{T}(正方形), 荧光光谱 S^{F}(圆形) 和水蒸气拉曼光谱 S^{V}(六边形) 的分解归一化光谱分量[99]

Fig.5　Total normalized spectra S^{T}(square) derived by the lidar using accumulated photons in 1.5–2.0 km altitude range, decomposed normalized spectral components of fluorescence spectra S^{F}(circle) and water vapor Raman spectra S^{V}(hexagon) [99]

2.2.2　大气中花粉、污染物等气溶胶的探测

2012 年, NIES 开发了一台 355 nm 激光雷达, 脉冲能量为 100 mJ, 重频为 30 Hz, 并使用 420~510 nm 范围内的总荧光信号来研究荧光生物气溶胶的分布。观测结果表明, 亚洲沙尘和一些空气污染气溶胶均能产生荧光, 这表明荧光测量可为气溶胶探测提供更加有用的信息[93]。

同年, Shinshu University 开发了一种紧凑型 LIF

激光雷达，对湖内蓝绿藻进行实时监测。该激光雷达所获取的数据与化学分析测定的蓝绿藻蛋白呈显著正相关关系[105]，为远程水质监测提供了新的解决方案[106]。2018 年，该研究组针对日本当地的花粉，建立了常见花粉的荧光光谱库，并利用激光雷达进行远程探测。实际测得的花粉光谱与光谱库中的数据较为吻合，如图 6 所示[53]。

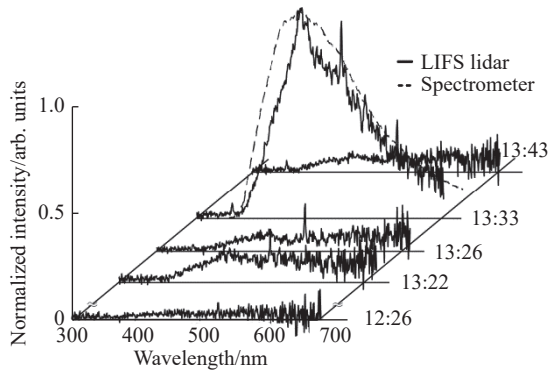

图 6 LIFS 激光雷达探测到空中杉树花粉的荧光光谱 (实线) 和光谱库中的荧光光谱 (虚线)，插图是实验现场[53]

Fig.6 Fluorescence spectra of Jpn. Cedar pollen in air (solid line) detected by the LIFS lidar and fluorescence spectrum in the spectral library (dashed line), inset shows the experimental site[53]

2020 年，ULille 的大气光学实验室与 GPI RAS 合作，搭建了一台米-拉曼-荧光激光雷达，通过 44 nm 带宽的积分光谱研究生物气溶胶的荧光[7]。在 2021 年法国花粉季节的观测实验中，该研究团队提出在较为干燥的环境下，荧光容量 (荧光与弹性后向散射系数之比) 才较为可靠[107]。2022 年，该研究团队成功反演出了卷云内烟雾的颗粒数量、表面积和体积浓度等重要信息[108]。此外，分析结果表明荧光为研究卷云内部的 BBA 粒子提供了重要信息[109]。同年 8 月，该研究团队结合 532 nm 退偏振比和荧光容量这两个参数尝试对气溶胶进行分类，并进行了大量的验证实验。荧光的加入，提高了激光雷达识别气溶胶粒子的能力[70]。2023 年，激光雷达的 355 nm 荧光接收通道增加至五个，经实验后认为不同荧光波长的比值具有识别气溶胶的潜力[97]。

2.2.3 生物战剂 (BWA) 的识别

自 2005 年起，隶属于 FFI 的“ARBC forsvar”项目开始建立生物气溶胶遥测系统[84]。2009 年，项目成功获得了枯草芽孢杆菌和苏云金芽孢杆菌的特征光谱，并证实了基于红外激光雷达的快速搜索能力的重要性[86]。2010 年，该系统还使用了光谱角度映射 (SAM) 算法，使用少于 20 个光谱通道的数据就对实验中施放的生物气溶胶进行了有效区分[110]。

同年，在之前 SINBAHD 激光雷达的基础上，加拿大 DRDC 启动了 BioSense 项目[111]。最初，该项目搭建了一台小型激光雷达 (SR-Biospectra)，并在实验中成功观测到了 100 m 处的低浓度生物气溶胶[112]。到 2011 年，BioSense 系统基本建成，能够在开阔空间执行国防军事任务，该系统搭载在卡车上，发射 355 nm 和 1.57 μm 的激光，并具备 360°扫描功能[78]。在 2012 年和 2015 年，该系统进行了多次实验，均迅速识别出了生物气溶胶模拟物并发出了报警信号[113-114]。图 7 展示了 DRDC 的车载式 BioSense 系统。

图 7 加拿大国防研究与发展部 (DRDC) 开发出的 BioSense 系统[113]

Fig.7 The Defense Research and Development Canada (DRDC) has developed the BioSense system[113]

2.3 其它单激发波长和多激发波长

1999 年，加拿大 DRDC 启动了一项名为 SINBAHD 的三年项目。该装置使用 351 nm 激光来激发荧光，单脉冲能量在 150~200 mJ 之间，重频为 125 Hz，使用 ICCD 采集生物气溶胶的荧光信号。从 2001 年至 2008 年，该系统进行了多次外场实验，成功获取了生物气溶胶模拟物、花粉和海洋气溶胶等多种生物气溶胶颗粒的荧光信息[56,115-119]。经过多次测试，SINBAHD 已发展成为一套成熟的生物气溶胶探测系统[111]。

2011 年，挪威 FFI 利用一种非线性光学过程，得到了 294 nm 的激光[120]。2012 年，该课题组使用 294 nm 和 355 nm 的激光对七种不同生物制剂的荧光光谱进行了测量。在实验中，较短波长 (294 nm) 激发

的光谱呈现出更明显的特征，但荧光光谱可能会受到大气成分拉曼散射的影响[52]。

2014 年，德国 DLR 搭建了 280 nm 和 355 nm 双激发波长的激光雷达，并结合一系列算法对不同类型的生物气溶胶进行了分类，获得了 92%~98% 的分类准确率[40]。2016 年，该研究小组对不同活性生物气溶胶的荧光光谱展开了测量[121]。2017 年，他们使用了更多种类的生物气溶胶进行测试，并采用机器学习等算法对荧光光谱进行了分类。图 8 展示了两种激发波长下不同生物气溶胶的荧光光谱，相较于 355 nm 而言，280 nm 激发产生的荧光光谱的可区分性更强[51]。2018 年，该研究团队使用 266 nm 和 355 nm 作为激发波长，并将荧光通道调整为 32 个，成功观测了三种不同细菌，决策树算法的分类正确率高达 98%[122]。2020 年，为了提高生物气溶胶荧光光谱的区分性，该研究小组还测量了单发射通道 (460 nm) 的荧光寿命，为生物气溶胶的探测增添了更多有价值的信息[48]。

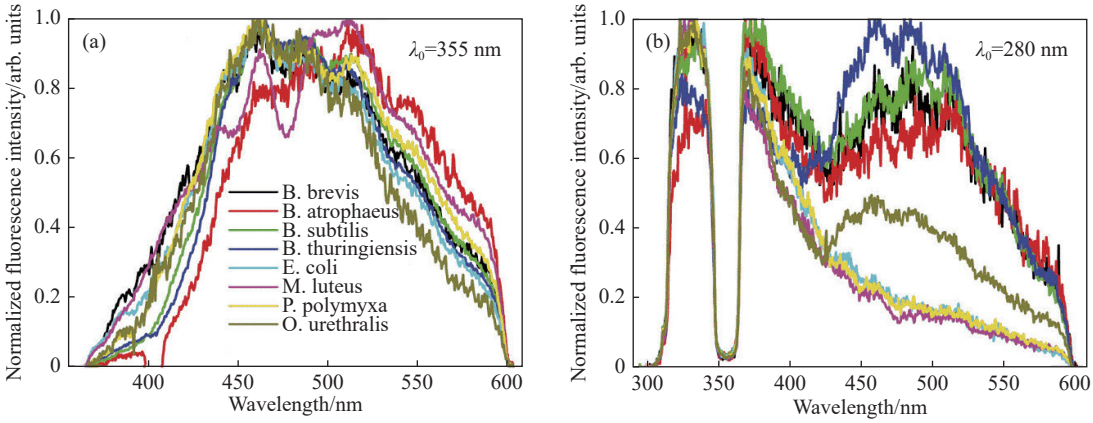

图 8　两种波长下激发的不同细菌样品的归一化 LIF 光谱。(a) 激发波长为 355 nm; (b) 激发波长为 280 nm[51]

Fig.8　Normalized LIF spectra of different bacterial samples excited at two wavelengths. (a) Excitation at 355 nm; (b) Excitation at 280 nm[51]

2015 年，波兰 MUT 研制了一台双波长 LIF 激光雷达系统，使用 266 nm 和 355 nm 作为荧光激发波长，并配备了 28 通道的 PMT 用于接收荧光信号。测试结果表明，该系统能够在约 700 米的距离内检测到几百 ppl 浓度的生物气溶胶模拟物。进一步研究表明，主成分分析法 (PCA) 可以有效区分生物气溶胶模拟物与干扰物，并且 28 个荧光探测通道均具有显著贡献[92]。2018 年，该研究团队还探讨了激光雷达在生物和化学危害识别领域的应用前景[123]。

2022 年，为了监测大型公共场所潜在的生物恐袭事件并及时发现恐怖威胁，北京 Bewhale 公司开发了一套结合 266 nm 和 355 nm 激光雷达以及无人机采样的综合系统。在对色氨酸气溶胶 (测试距离 200~800 m) 的实验中，该系统的识别正确率达到 70%[75]。

同年，日本 Shinshu University 使用商用的荧光光谱仪观测了 61 种已知气溶胶的 EEM 荧光光谱库，并基于 EEM 数据设计了 LIF 激光雷达[124]。该激光雷达使用四种波长 (520 nm、445 nm、405 nm 和 325 nm) 作为激发波长，将商用荧光光谱仪用于探测荧光光谱信号，并对雪松、豚草和苹果花粉进行了激发实验。结果表明，该激光雷达的测量结果与 EEM 光谱库的数据较为一致，多波长激发可显著提高生物气溶胶的鉴别能力[96]。

3　总　结

3.1　局限性

LIF 激光雷达是当前生物气溶胶远程探测领域中研究最为广泛的技术之一，能够实时获取生物气溶胶的特征光谱。在识别和区分近距离的生物气溶胶方面具有显著优势。然而，该技术也存在一些局限性：

1) 柴油烟雾等非生物气溶胶也可能产生荧光信号，给生物气溶胶的准确识别带来挑战，同时未知生物气溶胶的可识别性也需进一步验证。

2) 白天探测困难，多数系统仅局限于夜间探测，很难捕捉到白天的荧光信号，但是生物气溶胶的排放在白天更为频繁。

3) 紫外波段高能量激光对人眼构成威胁。有研究者使用了相对安全的低能量 405 nm 激光，但其性能还有待验证。

3.2 应用前景

随着研究的不断深入，LIF 激光雷达的探测性能正在持续提升。结合多种激发波长和分析算法 (如主成分分析、支持向量机、光谱角映射等) 的 LIF 激光雷达，在生物气溶胶的探测和识别方面展现出良好的应用前景，同时可与偏振、LIBS 和 DISC 等技术相结合，以获取更丰富的生物气溶胶遥测信息。LIF 激光雷达在生物气溶胶远程探测领域的应用前景主要集中在以下两个方面：

1) 长期大气环境监测系统：该类系统旨在实现长期稳定的气溶胶观测，主要通过荧光积分信号来对目标气溶胶进行分析。同时，结合退偏振比、拉曼和多通道弹性散射信号，可以更全面地描述气溶胶特征。但是此类系统得到的荧光信号并不能直接确定生物气溶胶种类和分布，因此亟需结合多种仪器进行长期观测，以探究荧光信号中的生物成分信息。目前，国内外已有多个研究团队成功构建了多波长激光雷达系统，并开展了相关监测工作。

2) 快速定位与识别生物战剂的系统：该系统侧重于快速、远距离定位并识别生物气溶胶，特别是生物战剂。此类系统一般通过红外弹性回波进行远距离气溶胶云定位，并结合紫外激发的荧光光谱和荧光光谱库进行近距离分析。该系统需要对多激发波长技术进行研究，并建立相应的荧光光谱库，以实现更精准、更高效的识别能力。国外已有研究者开发出相关系统并与原位仪器进行了大量协同测试，但是国内的相关研究尚显不足。

在空气污染、疫情爆发和生物恐怖袭击的背景下，以 LIF 技术为主的生物气溶胶激光雷达作为一种具有远距离、高速度、高精度的主动遥感探测手段，展示出巨大的应用潜力和发展前景。

参考文献：

[1] AMATO P, BRISEBOIS E, DRAGHI M, et al. Main Biological Aerosols, Specificities, Abundance, and Diversity [M]//DELORT A M, AMATO P. Microbiology of Aerosols. 1st ed. Hoboken, NJ: John Wiley & Sons, 2017: 1-21.

[2] DESPRÉS Vivianer, HUFFMAN J A, BURROWS S M, et al. Primary biological aerosol particles in the atmosphere: a review [J]. ***Tellus B: Chemical and Physical Meteorology***, 2012, 64(1): 15598.

[3] LÖNDAHL J. Physical and Biological Properties of Bioaerosols [M]//JONSSON P, OLOFSSON G, Tjärnhage T. Bioaerosol Detection Technologies. New York, NY: Springer New York, 2014: 33-48.

[4] DU R. The progress of atmospheric bioaerosol research [J]. ***Climatic and Environmental Research***, 2006, 11(4): 546-552. (in Chinese)

[5] MATTHIAS-MASER S, JAENICKE R. The size distribution of primary biological aerosol particles with radii > 0.2 μm in an urban/rural influenced region [J]. ***Atmospheric Research***, 1995, 39(4): 279-286.

[6] MAKI L R, GALYAN E L, CHANG-CHIEN M M, et al. Ice nucleation induced by pseudomonas syringae [J]. ***Applied Microbiology***, 1974, 28(3): 456-459.

[7] VESELOVSKII I, HU Q, GOLOUB P, et al. Combined use of Mie-Raman and fluorescence lidar observations for improving aerosol characterization: feasibility experiment [J]. ***Atmospheric Measurement Techniques***, 2020, 13(12): 6691-6701.

[8] SHI G Y, TAN S C, CHEN B. Environmental and climatic effects of mineral dust and bioaerosol [J]. ***Chinese Journal of Atmospheric Sciences***, 2018, 42(3): 559-569. (in Chinese)

[9] TANG D, WEI T, YUAN J, et al. Observation of bioaerosol transport using wideband integrated bioaerosol sensor and coherent Doppler lidar [J]. ***Atmospheric Measurement Techniques***, 2022, 15(9): 2819-2838.

[10] TANG S, MAO Y, JONES R M, et al. Aerosol transmission of SARS-CoV-2? Evidence, prevention and control [J]. ***Environment International***, 2020, 144: 106039.

[11] FENNELLY K P. Particle sizes of infectious aerosols: implications for infection control [J]. ***The Lancet Respiratory Medicine***, 2020, 8(9): 914-924.

[12] SOMSEN G A, VAN Rijn C, KOOIJ S, et al. Small droplet aerosols in poorly ventilated spaces and SARS-CoV-2 transmission [J]. ***The Lancet Respiratory Medicine***, 2020, 8(7): 658-659.

[13] KARIA R, GUPTA I, KHANDAIT H, et al. COVID-19 and its modes of transmission [J]. ***SN Comprehensive Clinical***

Medicine, 2020, 2(10): 1798-1801.

[14] JOSEPH J, BABY H M, ZHAO S, et al. Role of bioaerosol in virus transmission and material-based countermeasures [J]. *Exploration*, 2022, 2(6): 20210038.

[15] LAKE I R, JONES N R, AGNEW M, et al. Climate change and future pollen allergy in Europe [J]. *Environmental Health Perspectives*, 2017, 125(3): 385-391.

[16] HENDERSON D A. The looming threat of bioterrorism [J]. *Science*, 1999, 283(5406): 1279-1282.

[17] DANZIG R. Why should we be concerned about biological warfare? [J]. *JAMA: The Journal of the American Medical Association*, 1997, 278(5): 431-432.

[18] MAYOR S D, BENDA P, MURATA C E, et al. Lidars: A key component of urban biodefense [J]. *Biosecurity and Bioterrorism: Biodefense Strategy, Practice, and Science*, 2008, 6(1): 45-56.

[19] BOHLMANN S, SHANG X, GIANNAKAKI E, et al. Detection and characterization of birch pollen in the atmosphere using a multiwavelength Raman polarization lidar and Hirst-type pollen sampler in Finland [J]. *Atmospheric Chemistry and Physics*, 2019, 19(23): 14559-14569.

[20] SASSEN K. Boreal tree pollen sensed by polarization lidar: Depolarizing biogenic chaff [J]. *Geophysical Research Letters*, 2008, 35(18): 2008GL035085.

[21] MCDERMID I S. Ground-based lidar and atmospheric studies [J]. *Surveys in Geophysics*, 1987, 9(2): 107-122.

[22] DI H, HUA D, YAN L, et al. Polarization analysis and corrections of different telescopes in polarization lidar [J]. *Applied Optics*, 2015, 54(3): 389.

[23] BOHLMANN S, SHANG X, VAKKARI V, et al. Lidar depolarization ratio of atmospheric pollen at multiple wavelengths [J]. *Atmospheric Chemistry and Physics*, 2021, 21(9): 7083-7097.

[24] NOH Y M, LEE H, MUELLER D, et al. Investigation of the diurnal pattern of the vertical distribution of pollen in the lower troposphere using LIDAR [J]. *Atmospheric Chemistry and Physics*, 2013, 13(15): 7619-7629.

[25] YANG H, ZHAO X S, SUN Y F, et al. Bioaerosols polarization measurement by short-range multi-wavelength lidar [J]. ***Journal of Atmospheric and Environmental Optics***, 2018, 13(1): 52. (in Chinese)

[26] ROY G. Lidar polarization discrimination of bioaerosols [J]. *Optical Engineering*, 2010, 49(11): 116201.

[27] BROWN D M, THRUSH E, THOMAS M E. Chamber lidar measurements of biological aerosols [J]. *Applied Optics*, 2011, 50(5): 717.

[28] GOTTFRIED J L, DE LUCIA F C, MUNSON C A, et al. Laser-induced breakdown spectroscopy for detection of explosives residues: a review of recent advances, challenges, and future prospects [J]. *Analytical and Bioanalytical Chemistry*, 2009, 395(2): 283-300.

[29] CHIN S L, XU H L, LUO Q, et al. Filamentation “remote” sensing of chemical and biological agents/pollutants using only one femtosecond laser source [J]. ***Applied Physics B***, 2009, 95(1): 1-12.

[30] XU H L, MÉJEAN G, LIU W, et al. Remote detection of similar biological materials using femtosecond filament-induced breakdown spectroscopy [J]. *Applied Physics B*, 2007, 87(1): 151-156.

[31] GOTTFRIED J L. Discrimination of biological and chemical threat simulants in residue mixtures on multiple substrates [J]. *Analytical and Bioanalytical Chemistry*, 2011, 400(10): 3289-3301.

[32] GOTTFRIED J L, DE LUCIA F C, MUNSON C A, et al. Standoff detection of chemical and biological threats using laser-induced breakdown spectroscopy [J]. *Applied Spectroscopy*, 2008, 62(4): 353-363.

[33] GLENNON J J, NICHOLS T, GATT P, et al. System performance and modeling of a bioaerosol detection lidar sensor utilizing polarization diversity [C]///Proceedings of SPIE, 2009, 7323: 73230T.

[34] LAMBERT-GIRARD S, Hô N, BOURLIAGUET B, et al. Proposal for a standoff bio-agent detection SWIR/MWIR differential scattering lidar [C]//Proceedings of SPIE, 2012, 8358: 835805.

[35] THRUSH E, SALCICCIOLI N, BROWN D M, et al. Backscatter signatures of biological aerosols in the infrared [J]. *Applied Optics*, 2012, 51(12): 1836.

[36] WARREN R E, OSHER S J, VANDERBEEK R G. Multiple aerosol unmixing by the split bregman algorithm [J]. *IEEE Transactions on Geoscience and Remote Sensing*, 2012, 50(9): 3271-3279.

[37] KAYE P H, STANLEY W R, HIRST E, et al. Single particle multichannel bio-aerosol fluorescence sensor [J]. *Optics Express*, 2005, 13(10): 3583-3593.

[38] AN T, LIANG Z, CHEN Z, et al. Recent progress in online detection methods of bioaerosols [J]. *Fundamental Research*, 2024, 4(3): 442-454.

[39] PAN Y L. Detection and characterization of biological and other organic-carbon aerosol particles in atmosphere using

fluorescence [J]. ***Journal of Quantitative Spectroscopy and Radiative Transfer***, 2015, 150: 12-35.

[40] HAUSMANN A, DUSCHEK F, FISCHBACH T, et al. Standoff detection: classification of biological aerosols using laser induced fluorescence (LIF) technique [C]//Proceedings of SPIE, 2014, 9073: 90730Z.

[41] RAO Z, HE T, HUA D, et al. Preliminary measurements of fluorescent aerosol number concentrations using a laser-induced fluorescence lidar [J]. ***Applied Optics***, 2018, 57(25): 7211.

[42] SHANGGUAN M, LIAO Z, GUO Y. Simultaneous sensing profiles of beam attenuation coefficient and volume scattering function at 180° using a single-photon underwater elastic-Raman lidar [J]. ***Optics Express***, 2024, 32(5): 8189.

[43] SHANGGUAN M, GUO Y, LIAO Z. Shipborne single-photon fluorescence oceanic lidar: instrumentation and inversion [J]. ***Optics Express***, 2024, 32(6): 10204.

[44] SHANGGUAN M, GUO Y, LIAO Z, et al. Sensing profiles of the volume scattering function at 180° using a single-photon oceanic fluorescence lidar [J]. ***Optics Express***, 2023, 31(24): 40393.

[45] PALOMBI L, LOGNOLI D, RAIMONDI V. Fluorescence LIDAR remote sensing of oils: merging spectral and time-decay measurements [C]//Proceedings of SPIE, 2013, 8887: 88870F.

[46] PALOMBI L, ALDERIGHI D, CECCHI G, et al. A fluorescence LIDAR sensor for hyper-spectral time-resolved remote sensing and mapping [J]. ***Optics Express***, 2013, 21(12): 14736.

[47] LI X LONG, CHEN Y HUA, Li J, et al. Time-resolved fluorescence spectroscopy of oil spill detected by ocean lidar[C]//Proceedings of SPIE, 2016, 10155: 101550Q.

[48] FELLNER L, KRAUS M, GEBERT F, et al. Multispectral LIF-based standoff detection system for the classification of CBE hazards by spectral and temporal features [J]. ***Sensors***, 2020, 20(9): 2524.

[49] RICHARDSON S C, MYTILINAIOS M, FOSKINIS R, et al. Bioaerosol detection over Athens, Greece using the laser induced fluorescence technique [J]. ***Science of The Total Environment***, 2019, 696: 133906.

[50] SHOSHANIM O, BARATZ A. Daytime measurements of bioaerosol simulants using a hyperspectral laser-induced fluorescence LIDAR for biosphere research [J]. ***Journal of Environmental Chemical Engineering***, 2020, 8(5): 104392.

[51] DUSCHEK F, FELLNER L, GEBERT F, et al. Standoff detection and classification of bacteria by multispectral laser-induced fluorescence [J]. ***Advanced Optical Technologies***, 2017, 6(2): 75-83.

[52] FARSUND O, RUSTAD G, SKOGAN G. Standoff detection of biological agents using laser induced fluorescence —a comparison of 294 nm and 355 nm excitation wavelengths [J]. ***Biomedical Optics Express***, 2012, 3(11): 2964-2975.

[53] SAITO Y, ICHIHARA K, MORISHITA K, et al. Remote detection of the fluorescence spectrum of natural pollens floating in the atmosphere using a Laser-Induced-Fluorescence Spectrum (LIFS) lidar [J]. ***Remote Sensing***, 2018, 10(10): 1533.

[54] REICHARDT J, BEHRENDT O, LAUERMANN F. Spectrometric fluorescence and Raman lidar: absolute calibration of aerosol fluorescence spectra and fluorescence correction of humidity measurements [J]. ***Atmospheric Measurement Techniques***, 2023, 16(1): 1-13.

[55] BABICHENKO S, BENTAHIR M, PIETTE A, et al. Non-contact, real-time laser-induced fluorescence detection and monitoring of microbial contaminants on solid surfaces before, during and after decontamination [J]. ***Journal of Biosensors & Bioelectronics***, 2018, 9(2): 1000255.

[56] SIMARD J R, ROY G, MATHIEU P, et al. Standoff sensing of bioaerosols using intensified range-gated spectral analysis of laser-induced fluorescence [J]. ***IEEE Transactions on Geoscience and Remote Sensing***, 2004, 42(4): 865-874.

[57] YANG Z, LI C, YU M, et al. Compact 405-nm random-modulation continuous wave lidar for standoff biological warfare detection [J]. ***Journal of Applied Remote Sensing***, 2015, 9(1): 096042.

[58] BAXTER K, CASTLE M, BARRINGTON S, et al. UK small scale UVLIF lidar for standoff BW detection [C]//Proceedings of SPIE, 2007, 6739: 67390Z.

[59] JONSSON P, KULLANDER F. Bioaerosol Detection with Fluorescence Spectroscopy [M]//JONSSON P, OLOFSSON G, TJÄRNHAGE T. Bioaerosol Detection Technologies. New York, NY: Springer New York, 2014: 111-141.

[60] SCHÄFER F P. Principles of Dye Laser Operation [M]//SCHÄFER F P. Dye Lasers: Vol. 1. Berlin, Heidelberg: Springer Berlin Heidelberg, 1973: 1-85.

[61] PÖHLKER C, HUFFMAN J A, PÖSCHL U. Autofluorescence of atmospheric bioaerosols–fluorescent biomolecules and potential interferences [J]. ***Atmospheric Measurement Techniques***, 2012, 5(1): 37-71.

[62] RAO Zhimin. Detection technology and experimental research

of bioaerosol by fluorescent LiDAR in atmospheric boundary layer[D]. Xi′an: Xi′an University of Technology, 2018. (in Chinese)

[63] SAARI S E, PUTKIRANTA M J, KESKINEN J. Fluorescence spectroscopy of atmospherically relevant bacterial and fungal spores and potential interferences [J]. ***Atmospheric Environment***, 2013, 71: 202-209.

[64] HILL S C, MAYO M W, CHANG R K. Fluorescence of bacteria, pollens, and naturally occurring airborne particles: Excitation/emission spectra: ARL-TR-4722[R]. Adelphi, MD: U. S. Army Research Laboratory, 2009.

[65] PAN Y L, HUANG H, CHANG R K. Clustered and integrated fluorescence spectra from single atmospheric aerosol particles excited by a 263- and 351-nm laser at New Haven, CT, and Adelphi, MD [J]. ***Journal of Quantitative Spectroscopy and Radiative Transfer***, 2012, 113(17): 2213-2221.

[66] ZHANG W, Chen Q. Signal-to-noise ratio performance comparison of electron multiplying CCD and intensified CCD detectors [C]//2009 International Conference on Image Analysis and Signal Processing, 2009: 337-341.

[67] KUMAR D, SHARMA R C, MAINI A K. Standoff laser-induced fluorescence sensors for biological warfare agents [J]. ***Spectroscopy Letters***, 2013, 46(2): 147-153.

[68] PAN Y le, COBLER P, RHODES S, et al. High-speed, high-sensitivity aerosol fluorescence spectrum detection using a 32-anode photomultiplier tube detector [J]. ***Review of Scientific Instruments***, 2001, 72(3): 1831-1836.

[69] RAO Z, HUA D, HE T, et al. Ultraviolet laser-induced fluorescence lidar for pollen detection [J]. ***Optik***, 2017, 136: 497-502.

[70] VESELOVSKII I, HU Q, GOLOUB P, et al. Combining Mie–Raman and fluorescence observations: a step forward in aerosol classification with lidar technology [J]. ***Atmospheric Measurement Techniques***, 2022, 15(16): 4881-4900.

[71] JOSHI D, KUMAR D, MAINI A K, et al. Detection of biological warfare agents using ultra violet-laser induced fluorescence LIDAR [J]. ***Spectrochimica Acta Part A: Molecular and Biomolecular Spectroscopy***, 2013, 112: 446-456.

[72] SHIN J, NOH Y. Possible detection of atmospheric bioaerosol via LiDAR: a wavelength-based simulation study [J]. ***Asian Journal of Atmospheric Environment***, 2024, 18(1): 13.

[73] YANG H, ZHAO X S, SUN Y F, et al. Bio-agents and aerosol measurement by fluorescence and depolarization short-distance lidar [J]. ***Infrared and Laser Engineering***, 2017, 46(10): 1030004. (in Chinese)

[74] YANG H, MA X B, SUN Y F, et al. 2D fluorescence spectra measurement of 6 kinds of bioagents simulants by short-range lidar [J]. ***Spectroscopy and Spectral Analysis***, 2019, 39(3): 802-806. (in Chinese)

[75] WEI Y, WANG G Q, WANG X D, et al. Research on bioaerosol monitoring technology based on lidar and UAV [J]. ***China Port Science And Technology***, 2022, 4(7): 11-19. (in Chinese)

[76] CHEN S, CHEN Y, ZHANG Y, et al. Dual-channel mobile fluorescence lidar system for detection of tryptophan [J]. ***Applied Optics***, 2020, 59(3): 607.

[77] LI B, CHEN S, ZHANG Y, et al. Fluorescent aerosol observation in the lower atmosphere with an integrated fluorescence-Mie lidar [J]. ***Journal of Quantitative Spectroscopy and Radiative Transfer***, 2019, 227: 211-218.

[78] SIMARD J R, BUTEAU S, LAHAIE P, et al. BioSense/SR-BioSpectra demonstrations of wide area/early warning for bioaerosol threats: program description and early test and evaluation results[C]//Proceedings of SPIE, 2011, 8189: 81890E.

[79] KUMAR S, PARMAR A, SHARMA R C. Remote sensing of biochemicals in aerosol form using fluorescence sensor for defence and security [J]. ***IEEE Sensors Journal***, 2019, 19(23): 11129-11133.

[80] GUPTA L, SHARMA R C, RAZDAN A K, et al. Laser induced fluorescence of biochemical for UV LIDAR application [J]. ***Journal of Fluorescence***, 2014, 24(3): 709-711.

[81] HOPKINS R J, BARRINGTON S J, CASTLE M J, et al. UV-LIF lidar for standoff BW aerosol detection[C]//Proceedings of SPIE, 2009, 7484: 748409.

[82] IMMLER F, ENGELBART D, SCHREMS O. Fluorescence from atmospheric aerosol detected by a lidar indicates biogenic particles in the lowermost stratosphere [J]. ***Atmospheric Chemistry and Physics***, 2005, 5(2): 345-355.

[83] CHRISTESEN S D, MERROW C N, DESHA M S, et al. Ultraviolet fluorescence lidar detection of bioaerosols[C]// Proceedings of SPIE, 1994, 2222: 228-237.

[84] RUSTAD G, FARSUND Ø. Standoff detection of biological aerosols by UV-laser induced fluorescence: FFI-rapport 2008/02025[R]. Norwegian Defence Research Establishment (FFI), 2008.

[85] STEINVALL O, JONSSON P, KULLANDER F. Performance analysis for standoff biological warfare agent detection

lidar[C]//Proceedings of SPIE, 2007, 6739: 673912.

[86] JONSSON P, ELMQVIST M, GUSTAFSSON O, et al. Evaluation of biological aerosol stand-off detection at a field trial[C]//Proceedings of SPIE, 2009, 7484: 74840I.

[87] GRITSUTA A N, KLIMKIN A V, KOKHANENKO G P, et al. Mobile multi-wavelength aerosol lidar [J]. ***International Journal of Remote Sensing***, 2018, 39(24): 9400-9414.

[88] SHOSHANIM O, BARATZ A. A new fluorescence-based methodology for studying bioaerosol scavenging processes using a hyperspectral LIF-LIDAR remote sensing system [J]. ***Environmental Research***, 2023, 217: 114859.

[89] WANG Y, HUANG Z, ZHOU T, et al. Identification of fluorescent aerosol observed by a spectroscopic lidar over northwest China [J]. ***Optics Express***, 2023, 31(13): 22157.

[90] HUANG Z, WANG Y, ZHOU T, et al. Raman-Polarization-Fluorescence Spectroscopic Lidar for Real-Time Detection of Humic-like Substance Profiles [J]. ***Environmental Science & Technology***, 2025, 59(14): 7235-7245.

[91] SAKAI T, WHITEMAN D N, RUSSO F, et al. Liquid water cloud measurements using the raman lidar technique: current understanding and future research needs [J]. ***Journal of Atmospheric and Oceanic Technology***, 2013, 30(7): 1337-1353.

[92] WOJTANOWSKI J, ZYGMUNT M, MUZAL M, et al. Performance verification of a LIF-LIDAR technique for stand-off detection and classification of biological agents [J]. ***Optics & Laser Technology***, 2015, 67: 25-32.

[93] SUGIMOTO N, HUANG Z, NISHIZAWA T, et al. Fluorescence from atmospheric aerosols observed with a multi-channel lidar spectrometer [J]. ***Optics Express***, 2012, 20(19): 20800.

[94] LEE H S, HWANG I H, PRASAD C R. Portable digital lidar system: US6593582B2[P]. 2003-07-15.

[95] PRASAD C R, HUANG W, BUFTON J, et al. Low-power ultraviolet lidar for standoff detection of BW agents[C]//Proceedings of SPIE, 2004, 5416: 168-177.

[96] SAITO Y, KAWAI K. Initial experimental multi-wavelength EEM (Excitation Emission Matrix) fluorescence lidar detection and classification of atmospheric pollen with potential applications toward real-time bioaerosols monitoring [J]. ***Optics Express***, 2022, 30(11): 19922-19929.

[97] VESELOVSKII I, KASIANIK N, KORENSKII M, et al. Multiwavelength fluorescence lidar observations of smoke plumes [J]. ***Atmospheric Measurement Techniques***, 2023, 16(8): 2055-2065.

[98] TANG D, LI Z, XIA H. Clustering of weak fluorescence spectra from bioaerosol in air using laser-induced fluorescence lidar [J]. ***Optics Express***, 2025, 33(12): 24396-24412.

[99] LIU F, YI F, HE Y, et al. Spectrally resolved raman lidar to measure backscatter spectra of atmospheric three-phase water and fluorescent aerosols simultaneously: instrument, methodology, and preliminary results [J]. ***IEEE Transactions on Geoscience and Remote Sensing***, 2022, 60: 1-13.

[100] CHRISTESEN S D, WONG A, DESHA M S, et al. Ultraviolet-laser-induced fluorescence of aerosolized bacterial spores[C]// Proceedings of SPIE, 1993, 1885: 114-121.

[101] LEONARD D A, SHAW J F, SMITH C, et al. Compact hybrid IR/UV biological sensor[C]//Proceedings of SPIE, 1999, 3533: 164-173.

[102] SHOSHANIM O. Detection of bioaerosols using hyperspectral LIF-LIDAR during S/K challenge II campaign at Dugway [J]. ***Atmospheric Pollution Research***, 2023, 14(4): 101723.

[103] RAO Z M, HUA D X, HE T Y, et al. Research and analysis on lidar performance with intrinsic fluorescence biological aerosol measurements [J]. ***Acta Physica Sinica***, 2016, 65(20): 200701. (in Chinese)

[104] RAO Z M, HUA D X, HE T Y, et al. Design and simulation of laser induced bio-aerosols fluorescence lidar [J]. ***Acta Optica Sinica***, 2015, 35(10): 1028001. (in Chinese)

[105] SAITO Y, TAKANO K, KOBAYASHI F, et al. Development of a UV laser-induced fluorescence lidar for monitoring blue-green algae in Lake Suwa [J]. ***Applied Optics***, 2014, 53(30): 7030-7036.

[106] SAITO Y, KAKUDA K, YOKOYAMA M, et al. Design and daytime performance of laser-induced fluorescence spectrum lidar for simultaneous detection of multiple components, dissolved organic matter, phycocyanin, and chlorophyll in river water [J]. ***Applied Optics***, 2016, 55(24): 6727-6734.

[107] VESELOVSKII I, HU Q, GOLOUB P, et al. Mie–Raman–fluorescence lidar observations of aerosols during pollen season in the north of France [J]. ***Atmospheric Measurement Techniques***, 2021, 14(7): 4773-4786.

[108] VESELOVSKII I, HU Q, ANSMANN A, et al. Fluorescence lidar observations of wildfire smoke inside cirrus: a contribution to smoke–cirrus interaction research [J]. ***Atmospheric Chemistry and Physics***, 2022, 22(8): 5209-5221.

[109] HU Q, GOLOUB P, VESELOVSKII I, et al. The characterization of long-range transported North American biomass burning plumes: what can a multi-wavelength Mie–Raman-polarization-fluorescence lidar provide? [J].

Atmospheric Chemistry and Physics, 2022, 22(8): 5399-5414.

[110] FARSUND ø, RUSTAD G, KASEN I, et al. Required spectral resolution for bioaerosol detection algorithms using standoff laser-induced fluorescence measurements [J]. ***IEEE Sensors Journal***, 2010, 10(3): 655-661.

[111] JEAN-ROBERT S, SYLVIE B, PIERRE L, et al. Wide area spectrometric bioaerosol monitoring in Canada: from sinbahd to biosense [J]. ***International Journal of High Speed Electronics and Systems***, 2008, 18(3): 493-504.

[112] HÔ N, ÉMOND F, BABIN F, et al. Short-range lidar for bioagent detection and classification[C]//Proceedings of SPIE, 2010, 7665: 76650A.

[113] BUTEAU S, ROWSELL S. Biological material detection identification and monitoring: combining point and standoff sensors technologies[C]//Proceedings of SPIE, 2016, 9995: 99950B.

[114] BUTEAU S, SIMARD J R, ROY G, et al. Standoff detection of bioaerosols over wide area using a newly developed sensor combining a cloud mapper and a spectrometric LIF lidar[C]//Proceedings of SPIE, 2013, 8901: 890109.

[115] BUTEAU S, SIMARD J R, NADEAU D. Characterization of laser induced fluorescence from background aerosols in a maritime environment[C]//Proceedings of SPIE, 2011, 8018: 801803.

[116] BUTEAU S, SIMARD J R, ROY G. Standoff detection of natural bioaerosol by range-gated laser-induced fluorescence spectroscopy[C]//Proceedings of SPIE, 2005, 5995: 59950D.

[117] BUTEAU S, SIMARD J R, DÉRY B, et al. Bioaerosols laser-induced fluorescence provides specific robust signatures for standoff detection[C]//Proceedings of SPIE, 2006, 6378: 637813.

[118] BUTEAU S, SIMARD J R, ROWSELL S, et al. Bioaerosol standoff detection and correlation assessment with concentration and viability point sensors[C]//Proceedings of SPIE, 2010, 7838: 78380J.

[119] BUTEAU S, SIMARD J R, ROWSELL S. Bioaerosols standoff detection simultaneously refereed with particle concentration (ppl) and viability units (ACPLA)[C]//Proceedings of SPIE, 2009, 7484: 748408.

[120] FARSUND O, RUSTAD G. Sum-frequency generation of high-energy and high-beam-quality ultraviolet pulses [J]. ***International Journal of Optics***, 2011, 2011: 737684.

[121] WALTER A, DUSCHEK F, FELLNER L, et al. Application of Standoff LIF to living and inactivated bacteria samples[C]//Security Research Conference 11th Future Security Proceedings, 2016: 261-268.

[122] GEBERT F, KRAUS M, FELLNER L, et al. Novel standoff detection system for the classification of chemical and biological hazardous substances combining temporal and spectral laser-induced fluorescence techniques [J]. ***The European Physical Journal Plus***, 2018, 133(7): 269.

[123] WOJTANOWSKI J, ZYGMUNT M, KOPCZYŃSKI K, et al. Optical stand-off detection of biological and chemical hazards — Prospects and concerns[C]//2018 Baltic URSI Symposium (URSI), 2018: 100-105.

[124] SAITO Y, HOSOKAWA T, SHIRAISHI K. Collection of excitation-emission-matrix fluorescence of aerosol-candidate-substances and its application to fluorescence lidar monitoring [J]. ***Applied Optics***, 2022, 61(3): 653.

Research progress of bioaerosols fluorescence lidar technology

LI Zhekai[1], TANG Dawei[2], WU Kenan[1,2], WEI Tianwen[1], XIA Haiyun[1,2*]

(1. School of Atmospheric Physics, Nanjing University of Information Science and Technology, Nanjing 210044, China;
2. School of Earth and Space Science, University of Science and Technology of China, Hefei 230026, China)

Abstract:

Significance Bioaerosols are significant suspended particles in the atmosphere, such as pollens, viruses, and bacteria. They are widely dispersed due to atmospheric movement and have a considerable impact on human health and the environment. Lidar, as an advanced atmospheric remote sensing detection instrument, is well-suited for bioaerosols' remote detection due to its high sensitivity to atmospheric particles. Bioaerosols lidar can be applied to the early warning of biological warfare agents, real-time monitoring of pollen, and comprehensive atmospheric studies. A significant number of infections can be attributed to bioaerosols attacks. In order to implement effective countermeasures, it is essential to detect bioaerosols in the atmosphere with minimal delay. The current point detection methodology requires the collection of samples for subsequent laboratory analysis, which can take a period of 12 to 36 hours. In contrast, lidar-based detection presents a promising alternative. Based on the optical system, lidar enables real-time, long-distance detection and early warning, thereby allowing people to take action to prevent potential harm in a timely manner. In the context of pollen research, lidar is able to observe pollen in the atmosphere over a wide range, which is conducive to the study of pollen propagation and distribution patterns. Additionally, it can provide travel advice for individuals with pollen allergies and help assess pollen sensitization in the clinic. In the context of atmospheric research, ground-based lidar allows for long-term, stable observations, leading to the accumulation of substantial data, which supports statistical analyses of the spatial and temporal distribution of bioaerosols in the atmosphere.

Progress At present, Lidar for the remote detection of bioaerosols is founded upon four principal tenets: polarization, laser-induced breakdown spectroscopy (LIBS), differential scattering (DISC), and laser-induced fluorescence (LIF), LIF lidar is highlighted. Different fluorophores produce fluorescence spectra with different characteristics when excited by laser light. Therefore, it is theoretically possible to detect and distinguish fluorescent bioaerosols signals in the atmosphere at long distances by combining the LIF principle with a lidar system that emits laser light of a certain wavelength and receives fluorescent signals within a specific band. The wavelength is one of the most important factors affecting the performance of LIF lidar. Then different wavelengths of LIF lidar are analyzed (Tab.1), which need to take into account the fluorescence properties of the target substance. The LIF lidar can be categorized into two primary wavelength bands: one is mainly to excite the fluorescence of specific aromatic amino acids (under 300 nm), while the other is mainly to excite the molecules related to biological metabolism (above 300 nm). Due to the need for mature and reliable lasers for practical applications, most researchers have chosen 266 and 355 nm wavelengths, although some have used 294 nm in order to minimize ozone attenuation. Different photodetectors are also discussed. The LIF lidar bioaerosols detection-related research institutions are marked on a world map provided by the Standard Map Service system (Fig.3), and a list of lidar parameters is also given (Tab.2). After that, the article is divided into 266 nm single-wavelength-excited lidar, 355 nm single-wavelength-excited lidar, other single-wavelength-excited lidar and multi-wavelength-excited lidar to be described. 266 nm-excited lidar is mostly used in the detection of biological

warfare agents, which has a high variability of the excitation spectrum, but the detection distance is not far due to the strong absorption of ozone. But as in Fig.4, bioaerosols signals were detected by some researchers at 2.5km during the daytime. 355 nm-excited lidar has been applied to the following aspects: water vapor Raman signals interferes with fluorescence (Fig.5), and some research groups have proposed some optimization algorithms based on the fluorescence principle; 355 nm receives less interference in the air, so many research groups use it to detect long-distance bioaerosols fluorescence signals, and they have built up multi-wavelength lidars, which can detect the integral fluorescence signals of some air pollutants and pollens; also, some research groups have experimented with the ability to detect biological warfare agents and pollens (Fig.6) using bioaerosols fluorescence spectrum. Less research has been done on other wavelengths, but a number of researchers have demonstrated that multi-wavelength lidar provides rich spectral data and has great potential for bioaerosols identification.

Conclusions and Prospects The characteristics as well as limitations of LIF lidar bioaerosols technology are summarized. The well-performing designs are highlighted for the two types of systems: lidar systems intended for long-term stable atmospheric monitoring and those designed for the rapid identification of biological warfare agents, respectively. In the context of air pollution, epidemic outbreaks, and bioterrorism, bioaerosols lidar, based on LIF technology, has great potential for development as a means of detection with long range, high speed, and remarkable accuracy.

Key words: bioaerosols; lidar; atmospheric remote sensing; laser induced fluorescence